EUROPHYSICS LETTERS 1 November 1989
Europhys. Lett., **10** (5), 451-456 (1989)

Convective Patterns in Horizontal Flow.

H. W. MÜLLER (*), M. LÜCKE (*) and M. KAMPS (**)
(*) *Institut für Theoretische Physik, Universität des Saarlandes D-6600 Saarbrücken*
(**) *Institut für Festkörperforschung, Kernforschungsanlage Jülich - D-5170 Jülich*

(received 18 July 1989; accepted 25 August 1989)

PACS. 47.25Q – Convection and heat transfer.
PACS. 47.60 – Flows in ducts, channels, and conduits.

Abstract. – Rayleigh-Bénard convection in the presence of a horizontal throughflow perpendicular to the convective roll chain is investigated with a 1*d* amplitude equation and with a 2*d* numerical simulation of the basic hydrodynamic equations. Results agree very well with each other. The flow leads to propagating convective patterns in the form of travelling wave states which for increasing flow are localized further and further downstream. Unique wave number selection is observed. Related experiments are discussed.

An interesting pattern forming nonlinear system is the Rayleigh-Bénard problem subject to a lateral throughflow [1]. Here we report how the stationary convective roll chain in this system is changed when a lateral flow is imposed perpendicular to the roll axes, say in a long narrow channel heated from below. Then the onset of convection is delayed [1] and, more importantly, it becomes oscillatory with a forward Hopf bifurcation to a stable travelling wave (TW) state where the roll pattern propagates downstream. Hopf frequency, phase velocity, and group velocity grow for small flow rates linearly with the associated Reynolds number Re and can be tuned externally. For inlet conditions that suppress convection a stationary confined TW state [2] is formed that is localized closer and closer to the outlet with increasing Re. The downstream distance l that this state requires to grow from the inlet diverges at a particular Re^*. There the group velocity reaches the threshold value v_g^* which marks the borderline between absolute and convective instability [3]. Upon crossing this borderline by increasing Re or decreasing the Rayleigh number, Ra, any convective pattern is «blown» out of the system. Furthermore we observed in our simulations a unique wavelength selection: the flow-induced TW patterns depend only on the final Re-Ra combination but not on initial configurations or history. Finally we have also investigated patterns under phase pinning boundary conditions and thereby reproduced the experimental results of Pocheau *et al.* [4].

Consider a horizontal layer of an incompressible Boussinesq fluid that is heated from below between rigid perfectly conducting plates at $z = 0, 1$ with a lateral flow imposed in x-direction. Then, in the absence of convection the basic conductive state is homogeneous in x with a linear temperature profile $T_{\text{cond}}(z) = T_0 + Ra(1 - z)$ and a plane parabolic Poiseuille velocity field $U(z) = 6\sigma\, Re\, z(1-z)\, e_x$. Here $Ra = \alpha g d^3 \Delta T/(\varkappa\nu)$ is the Rayleigh number given in terms of thermal expansion coefficient α, gravitational constant g, layer thickness d, applied temperature difference ΔT, thermal diffusivity $\varkappa$, and kinematic viscosity ν. The second control parameter is the Reynolds number $Re = \bar{U}d/\nu$ measuring the spatial mean $\bar{U}$ of the laterally flow and the Prandtl number $\sigma = \nu/\varkappa$ is a material parameter. We scale lengths by d, times by $d^2/\varkappa$, and temperature by $\varkappa\nu/(\alpha g d^3)$.

For laterally infinite layers one expects from linear stability analyses [1] that the convective rolls to grow first would be oriented parallel to U (longitudinal rolls). However, in narrow rectangular ducts of dimension $L_x \gg L_y$ the sidewall forcing that favours transverse rolls with axes perpendicular to the long walls dominates and transverse rolls grow above onset provided that the throughflow is not too strong [5, 6]. We are considering here an idealized situation where long sidewalls indeed are necessary to enforce transverse rolls with axes parallel to y but where a two-dimensional description in an x-z cross-section is appropriate. Thus we take the convective fields of temperature θ and velocity $\boldsymbol{u} = (u, 0, w)$ to depend only on x, z, and t.

Lateral throughflow with small Re stabilizes the conductive state. The upwards shift [6-8] (1) of the stability threshold for onset of transverse convective rolls is $\sim Re^2$ and rather small, at least for $\sigma = 1$. In fig. 1 we show the critical value, $\varepsilon_c(Re)$, of the reduced Rayleigh

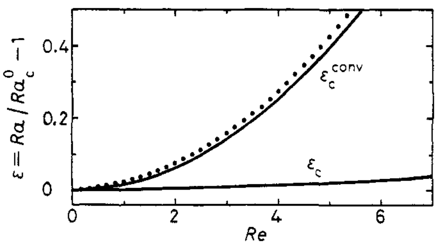

Fig. 1. – The basic conductive state is stable below the linear stability threshold ε_c, convectively unstable for $\varepsilon_c < \varepsilon < \varepsilon_c^{conv}$, and absolutely unstable for $\varepsilon_c^{conv} < \varepsilon$. At ε_c^{conv} or, equivalently, Re^* the streamwise growth length l of transverse convective rolls diverges. For $\varepsilon > \varepsilon_c^{conv}$ or $Re < Re^*(v_g < v_g^*)$ l is finite—cf. text. At the dotted line $l = 10$. Curves are parabolic for small Re.

number $\varepsilon = Ra/Ra_c^0 - 1$ that we have evaluated with a shooting method. Here $Ra_c^0 = 1707.76$ is the critical Rayleigh number without flow. With throughflow the instability of the conductive state is oscillatory with a Hopf frequency, ω_c, that increases $\sim Re$ for small Re. Therefore, close to the Hopf bifurcation threshold, $\varepsilon_c(Re)$, the fields $\phi = u, w, \theta$ have the form

$$\phi(x, z, t) = [A(x, t)\, \hat{\phi}(z) \exp[i(k_c x - \omega_c t)] + \text{c.c.}]\,. \tag{1}$$

Here $\hat{\phi}(z)$ is given by the eigenvector [8] of the linear stability problem at threshold. The

(1) For $\sigma = 1$ we got [8]: $Ra_c = 1707.76 + 1.32\, Re^2$ (we think there is an error in [7]), $k_c = 3.1163 + 10^{-4} Re^2$, $\tau_0 = 0.0769 - 5.004 \cdot 10^{-5} Re^2$, $\xi_0^2 = 0.148 - 1.044 \cdot 10^{-4} Re^2$, $\gamma = 0.703 - 5.04 \cdot 10^{-5} Re^2$, $\omega_c/k_c = 1.17 Re$, $v_g = 1.23 Re$. Note that $c_0 = 0.00704 Re$, $c_1 = -0.0181 Re$, and $c_2 = 0.0113 Re$ are small compared to 1 for our Re values.

complex amplitude, $A(x, t)$, of the convective roll pattern is given by the solution of the Ginzburg-Landau equation [9]

$$\tau_0(\partial_t + v_g \partial_x) A = [\mu(1 + ic_0) + (1 + ic_1) \xi_0^2 \partial_x^2 - \gamma(1 + ic_2)|A|^2] A . \tag{2}$$

Equations (1), (2) result [8] from a systematic expansion around threshold. The expansion parameter is $\sqrt{\mu}$ where

$$\mu = \frac{Ra}{Ra_c(Re)} - 1 = \frac{\varepsilon - \varepsilon_c(Re)}{1 + \varepsilon_c(Re)} \tag{3}$$

measures the reduced distance of Ra to the actual stability threshold $Ra_c(Re)$. The coefficients τ_0, ξ_0^2, γ have small corrections $\sim Re^2$ to their $Re = 0$ values, while ω_c and the group velocity at threshold, v_g, grows $\sim Re$ from zero with a correction $\sim Re^3$ as do the coefficients c_0, c_1, c_2 [8] ([1]). Note that γ, c_2 result from a nonlinear analysis.

In an experimental situation where the amplitude A of the rolls vanishes at the inlet, *e.g.*, a porous plug [6], one has to consider the growth of localized rather than extended convective perturbations. Invoking this concept [3] one finds that the conductive state, $A \equiv 0$, is convectively unstable for

$$0 < \mu < \mu_c^{\text{conv}} = \tau_0^2 v_g^2 / [4\xi_0^2(1 + c_1^2)] ; \qquad \varepsilon_c < \varepsilon < \varepsilon_c^{\text{conv}} = \varepsilon_c + (1 + \varepsilon_c) \mu_c^{\text{conv}} . \tag{4}$$

In this range localized perturbations are carried away with the throughflow so that rolls cannot grow globally. However, if $\varepsilon > \varepsilon_c^{\text{conv}}$ the conductive state is absolutely unstable: perturbations can grow and expand upstream until nonlinear saturation occurs. Then the final convective roll structure (cf. fig. 2) has a *stationary intensity envelope* that increases monotonously from the inlet with a characteristic growth length l, while the roll *pattern propagates downstream* with a stationary phase velocity. This we found by numerically solving for several ε, Re i) the amplitude equation and ii) the full two-dimensional hydrodynamical equations using an explicitly time-dependent finite difference MAC algorithm [10]. In both cases the conductive state was enforced at inlet $x = 0$ and outlet $x = 25$ by imposing $A = 0$ or $T_{\text{cond}}(z)$, $\boldsymbol{U}(z)$ there. Thin lines in fig. 2 show snapshots of the vertical velocity field $w(x, z = 0.5)$ as obtained from the numerical simulation of the full hydrodynamic equations. Thick lines show stationary envelopes resulting from the final state solution of (2) which we found [8] to be of the form $A(x, t) = B(x) \exp[i\Omega t]$.

In an infinite system the long-time solution of (2) would be spatially homogeneous $|B_\infty| = \sqrt{\mu/\gamma}$ with $\Omega_\infty = (c_0 - c_2)\mu/\tau_0$. Also in the finite system the correction Ω to ω_c remains very small. Thus the phase velocity is practically ω_c/k_c. However, the boundary conditions and the throughflow-generated group velocity give rise to envelope profiles [2] that are pushed more and more towards the outlet with increasing Re or v_g, respectively. The growth length l over which the stationary amplitude increases from the inlet to half the bulk value diverges (in a semi-infinite system) at a Reynolds number Re^* for which the group velocity reaches the value $v_g = v_g^* := 2\sqrt{\mu(1 + c_1^2)}\, \xi_0/\tau_0$. That happens in the Re-Ra plane of fig. 1 just at the convective threshold $\mu = \mu_c^{\text{conv}}$ or $\varepsilon = \varepsilon_c^{\text{conv}}$, respectively. Thus increasing Re beyond Re^* or decreasing Ra below Ra_c^{conv} will «blow» an initially present convective structure completely out of the system. We also mention the interesting relation: for a group velocity v_g^* the front propagation velocity [11] of a travelling pattern just becomes zero leading to a stationary front whose leading head ($B = 0$) is at $x = 0$ instead of being at $x = -\infty$.

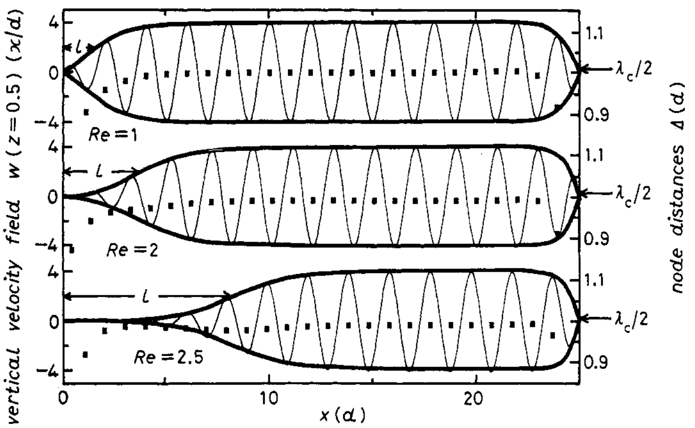

Fig. 2. – Snapshots of convective structures ($\varepsilon = 0.114$, $\sigma = 1$) after transients have died out. Thin lines show vertical velocity, $w(x, z = 0.5)$, at mid height of the layer from simulation of full hydrodynamic equations. Extrema mark positions of maximal up and down flow between adjacent rolls. Nodes coincide with roll centres. Rolls move downstream such that envelope and phase velocity is stationary. Full lines result without fit from the amplitude eq. (2) and linear eigenfunction $\hat{w}(z)$ at threshold. Boundary conditions at inlet, $x = 0$, and outlet, $x = 25$, suppress convection. The amplitude grows over a length l to half the bulk value. Local node distances, $\Delta(x)$, (squares) are smaller than half the critical wavelength (arrows) at ε_c.

In fig. 3 we show l *vs.* v_g as obtained from (2) and from our simulation for various Ra and Re. With the scaling $L = \sqrt{\mu} l/\xi_0$ and $V_g = [\mu(1 + c_1^2)]^{-1/2} v_g \tau_0/\xi_0$ all simulation data fall onto the line of the amplitude equation since the coefficients c_0, c_1, c_2 remain small for our Re. The rapid increase of l close to v_g^* or $\varepsilon_c^{\text{conv}}$ is reflected in fig. 1 by the dotted line for $l = 10$ being very close to the $l = \infty$ line $\varepsilon_c^{\text{conv}}$.

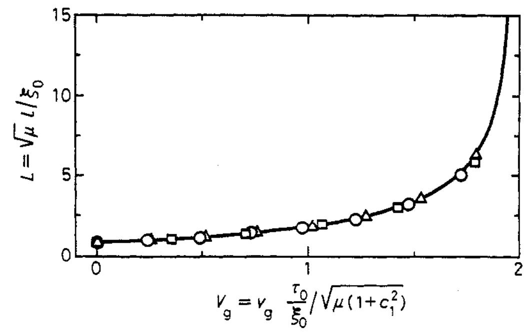

Fig. 3. – Reduced growth length L of transverse rolls *vs.* scaled group velocity V_g. Line results from the amplitude equation. All open symbols from simulating the full hydrodynamic equations for different $\varepsilon = 0.114$ and $Re \leqslant 2.5$ (circles), $\varepsilon = 0.215$ and $Re \leqslant 3.4$ (squares), $\varepsilon = 0.417$ and $Re \leqslant 4$ (triangles) fall onto the line. A fit shows a divergence $L \simeq 2.31(V_g^* - V_g)^{-0.637}$ near $V_g^* = 2$.

Confined states are also observable in the convectively unstable region (4) when a *permanent* source of disturbances is supplied, for example, a small noise source at $x = 0$ to simulate inlet turbulence. Then perturbations are amplified downstream and «noise sustained» convective states appear [12]. However, in the absolutely unstable domain, $\varepsilon > \varepsilon_c^{\text{conv}}$, the system is less sensitive to these disturbances [3].

In our simulations we found that a finite throughflow uniquely selects a pattern. Its bulk wavelength is independent of aspect ratio, initial configuration, and history. It depends only on the final *Re*-*Ra* combination and λ decreases weakly with growing *Re* and *Ra* (cf. fig. 4). With the amplitude of the rolls vanishing at inlet and outlet there is no phase pinning there. Thus the bulk wavelength of the downstream travelling pattern is free to be selected by an as yet unknown mechanism. However, the amplitude variation near inlet and outlet causes a characteristic local λ variation (cf. squares in fig. 2) which, by the way, is not properly reproduced by the amplitude equation.

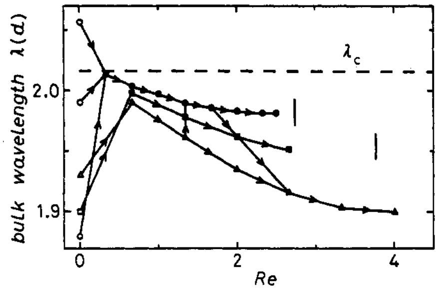

Fig. 4. – Bulk wavelengths selected in simulation runs (circles: $\varepsilon = 0.114$, squares: $\varepsilon = 0.215$, triangles: $\varepsilon = 0.417$). At $Re = 0$ states with different λ were prepared in systems of different lengths. Full symbols show wavelengths selected in the presence of flow and arrows indicate simulation protocols. For the lowest ε-values Re^* is marked by vertical lines.

In good qualitative agreement with our results are experiments [6] in a long narrow channel. For very small flow rate a propagating pattern of transverse rolls filled the whole box whereas it was confined to the outlet region for higher *Re*. Also the experimental ratio of phase velocity to mean flow velocity $v_{\text{phase}}/\bar{U} = 1.38$ compares well with a leading-order *Re*-expansion [7, 8] that yields at onset $v^c_{\text{phase}}/\bar{U} = (0.814\sigma + 0.279)/(0.618\sigma + 0.316)$. For $\sigma = 450$ [6] this is 1.32.

The experiments of Pocheau *et al.* [4] used azimuthally opposite flow in two halves of an annular container: phase pinning occurred in particular at the outlet where rolls were pushed against each other by the two counterflows. Thus for very small *Re* the pattern did not travel but was deformed with compressed (dilated) rolls near outlet (inlet). This was explained [4] in terms of phase diffusion. Only for larger *Re* occurred pattern propagation in the bulk. We have simulated this phase-pinning situation with von Neumann conditions, $\partial_x w = \partial_x T = 0$, at inlet and outlet and reproduced [8] the stationary experimental λ variation [4]. Our pattern begins to travel in the bulk at $Re \simeq 0.015$ for $\sigma = 1$. We also investigated phase pinning with the amplitude eqs. (1), (2) by setting $\tilde{A}(x, t) = A(x, t) \exp[-i\omega_c t]$ for small ω_c. Amplitude and phase variation of the stationary solution, $\tilde{A}(x)$, agreed perfectly with the corresponding simulations.

* * *

Discussions with J. K. PLATTEN are gratefully acknowledged. This work was supported by Volkswagen-Stiftung.

REFERENCES

[1] For a review see R. E. KELLY, in *Physicochemical Hydrodynamics*, edited by D. SPAULDING (Advanced Publ.) 1977, p. 65.
[2] CROSS M. C., *Phys. Rev. Lett.*, 57 (1986) 2935; *Phys. Rev. A*, 38 (1988) 3593.

[3] HUERRE P., in *Instabilities and Nonequilibrium Structures*, edited by E. TIRAPEGUI and D. VILLARROEL (D. Reidel Publishing Company, Dordrecht) 1987, p. 141 and references cited therein; CHOMAZ J. M., HUERRE P. and REDEKOPP L. G., *Phys. Rev. Lett.*, **60** (1988) 25.
[4] POCHEAU A., CROQUETTE V., LE GAL P. and POITOU C., *Europhys. Lett.*, **3** (1987) 915.
[5] PLATTEN J. K. and LEFEBVRE M., *Physica*, **51** (1971) 330.
[6] LUIJKX J. M., PLATTEN J. K. and LEGROS J. C., *Int. J. Heat Mass Transfer*, **24** (1981) 1287; LUIJKX J. M., Doctoral thesis (Université de l'Etat à Mons, Belgium) 1983.
[7] WALTON I. C., *Q. J. Mech. Appl. Math.*, **38** (1985) 561.
[8] MÜLLER H. W., LÜCKE M. and KAMPS M., unpublished.
[9] NEWELL A. C., in *Propagation in Systems far from Equilibrium*, edited by J. E. WESFREID, H. R. BRAND, P. MANNEVILLE, G. ALBINET and N. BOCCARA (Springer, Berlin) 1988 and references cited therein.
[10] HIRT C. W., NICHOLS B. D. and ROMERO N. C., Los Alamos Scientific Laboratory Report LA-5852 (1975); LÜCKE M., MIHELCIC M., KOWALSKI B. and WINGERATH K., in *The Physics of Structure Formation: Theory and Simulation*, edited by W. GÜTTINGER and G. DANGELMAYR (Springer, Berlin) 1987.
[11] NIKLAS M., LÜCKE M. and MÜLLER-KRUMBHAAR H., *Europhys. Lett.*, **9** (1989) 237.
[12] DEISSLER R. J., *J. Stat. Phys.*, **54** (1989) 1459 and references cited therein.